Screened Coulomb Pair Potential in Colloidal Interactions in Suspensions Revisited

K. S. Schmitz,*,† Arup K. Mukherjee,‡ and L. B. Bhuiyan‡

Department of Chemistry, University of Missouri-Kansas City, Kansas City, Missouri 64110 and Laboratory of Theoretical Physics, Department of Physics, University of Puerto Rico, Box 23343, UPR Station, San Juan, Puerto Rico 00931-3343

Received: December 19, 2002; In Final Form: June 19, 2003

Although the Derjaguin−Landau−Verwey−Overbeek (DLVO) -screened Coulomb pair interaction potential was derived under restricted theoretical conditions, its current usage on real systems tends to ignore these constraints, and consequently, the concepts of "effective charge", "effective screening parameter", and even "effective radius" have been championed in order to maintain the intrinsic DLVO mathematical form. The screened Coulomb expression is examined critically vis-à-vis the effective screening parameter for a charge stabilized colloidal suspension under salt-free conditions. Because the ion concentration under actual experimental conditions is usually unknown, or at best not reported, we simulate the experimental data by means of accurate Monte Carlo simulation methods, which enables one to control both the charge on the macroion and the microion concentration in the computation cell. These data are then fit to the standard Yukawa potential for the macroion as employed in the DLVO theory. It is seen that at low to moderate macroion charge ($\leq$400 $|e|$ for monovalent counterions, $\leq$150 |e| for divalent counterions) a "single" screened pairwise interaction between the macroion and the counterion is adequate. However, such analysis fails significantly for highly charged macroions.

1. Introduction

For the past half century or so, the stability of charged colloidal systems has generally been described in terms of the DLVO (Derjaguin−Landau−Verwey−Overbeek) potential between two colloidal particles. The DLVO potential is composed of a long-range screened Coulomb repulsion part ($U_{\mathrm{DLVO}}^{\mathrm{elec}}$) and a short-range van der Waals attraction part (U_{vdW}). What is of interest in the present study is the screened Coulomb contribution so the van der Waals contribution is omitted in what follows. The expression for $U_{\mathrm{DLVO}}^{\mathrm{elec}}$ between two identical macroions of charge Z_{p} and radius a_{p} separated by a center-to-center distance r thus obtained is

$$\beta U_{\mathrm{DLVO}}^{\mathrm{elec}} = \lambda_B Z_{\mathrm{p}}^{\ 2} \frac{\exp(2\kappa a_{\mathrm{p}})}{(1+\kappa a_{\mathrm{p}})^2} \frac{\exp(-\kappa \mathrm{r})}{\mathrm{r}} \qquad (1)$$

Although the DLVO potential was derived under very specific conditions to validate linearized solutions to the Poisson−Boltzmann equation, the application of eq 1 to experimental data has not been so constrained. Application of eq 1 under experimental conditions outside the range of its theoretical validity led to the concept of "effective" parameters for the macroion charge, Z_{eff}, and the screening length, κ_{eff}. Such empirical fits led at times to values of Z_{eff} considerably smaller than the "expected" value Z_{p}. Roberts, O'Dea, and Osteryoung[1] tabulated values of the ratio $Z_{\mathrm{eff}}/Z_{\mathrm{p}}$ as a function of $|Z_{\mathrm{p}}|/a_{\mathrm{p}}$. Their tabulation indicated that Z_{eff} may be smaller than Z_{p} by an order of magnitude or more for $|Z_{\mathrm{p}}|/a_{\mathrm{p}}$ greater than 200 nm^{-1}. The observation that $Z_{\mathrm{eff}}/Z_{\mathrm{p}} < 1$ stimulated many theoretical investigations to "justify" this result through some mathematical prescription.[2−10] Although the various methods for determination of the "effective" or "renormalized" charge may differ, they all agree on the concept that there are a certain number of "bound" counterions in the vicinity of the macroion surface, which forms a thermodynamically defined macroion-counterion unit of charge Z_{eff}. As noted by Ulander, Greberg, and Kjellander[11] in regard to the topic of effective charges:

"The key idea is to maintain the feature from above that the propagation of electrostatic potential in the electrolyte is governed by the screened Coulomb potential $\phi^{o}(r)$."

Although there has been ample activity in attempts to impart "physical content" in the numerical value of Z_{eff}, there is a noticeable absence of such activity directed to κ_{eff}. One such study was by Stevens, Falk, and Robbins[3], in which they compared the osmotic pressure obtained from Monte Carlo (MC) methods to that of the Debye−Hückel (DH) model. They found that the latter was in reasonable agreement with the former if a "renormalized" charge was used for the macroion. However, they did not correlate the effective charge with the screening parameter through a screened Coulomb pair potential of the microions with the macroion. However worthy it might seem to justify an effective charge for the primary purpose of retaining the screened Coulomb potential form of the pairwise interaction, the activity may prove empty if the physical content of κ (or κ_{eff}) is compromised.

It is not necessary to determine the pair interaction between two macroions in the simulation if the focus is on the screening parameter. This is because the DLVO pair potential is based on a superposition of the potential $\varphi(r)$ for the isolated macroion-microion, and therefore κ is the same for both types of potentials. We therefore employ MC simulations of the counterion distribution function about their parent macroion as the "standard" to establish if any relationship between the least-squares fit parameters Z_{eff} and κ_{eff} and the MC parameters Z_{p} and n_{c}.

* To whom correspondence should be addressed. E-mail: schmitzks@umkc.edu.
† University of Missouri-Kansas City.
‡ University of Puerto Rico.

10.1021/jp0226329 CCC: $25.00 © 2003 American Chemical Society
Published on Web 08/26/2003

2. Mathematical Forms of the Screening Parameter

We introduce the subject of study through the monumental work by Verwey and Overbeek,[12] in which the suspension of colloidal particles is sufficiently dilute that one need only consider the interaction between two colloidal particles. The potential $\Phi(\boldsymbol{r})$ at any location $\boldsymbol{r}$ in the solvent medium is simply the superposition of the screened Coulomb potentials for each of the two colloidal particles, which in symbolic form is given by

$$\Phi(r) = F(\varphi_1(r_1), \varphi_2(r_2)) \tag{2}$$

where $F(...)$ is a function whose form depends both on the angles and the distance of the potential contributions of each colloidal particle and the arguments of $F(...)$ are the potentials $\varphi_1(r_1)$ and $\varphi_2(r_2)$ given to be of the Yukawa form

$$\varphi_1(r_1) = \frac{Z_1\lambda_B \exp(-\kappa r_1)}{r_1}$$

$$\varphi_2(r_2) = \frac{Z_2\lambda_B \exp(-\kappa r_2)}{r_2} \tag{3}$$

In eq 3, r_1 and r_2 are the distances of particle 1 of charge Z_1 and particle 2 of charge Z_2, respectively, to the location $\boldsymbol{r}$, and $\lambda_B = \beta e^2/4\pi\epsilon_0\epsilon_r$ is the Bjerrum length where $|e|$ is the magnitude of the electron charge, ϵ_0 is the vacuum permeability, ϵ_r is the relative permeability, $\beta = 1/k_B T$, k_B is the Boltzmann constant and T, the absolute temperature. The parameter κ is the reciprocal screening length whose value determines the rate at which the electrostatic interaction decays with distance. The explicit form of κ is delayed until later.

There appears to be no general consensus as to the theoretical expression for the screening parameter κ. In his model for unipolar coacervates, Langmuir[13] treated the macroion as a point particle and defined κ as

$$\kappa^2 = 4\pi\lambda_B(Z_p^2 n_p + Z_c^2 n_c) = \kappa_p^2 + \kappa_c^2 = \kappa_L^2 \tag{4}$$

where n_p and n_c are the number concentration of the macroion and counterion, respectively, and Z_c is the counterion charge. The counterion contribution is related to the macroion concentration by

$$\kappa_c^2 = 4\pi\lambda_B Z_c^2 n_c = 4\pi\lambda_B Z_c^2 |Z_p| n_p \tag{5}$$

This is the same definition of κ employed recently by Chan, Linse, and Petris[14] in their model for colloidal systems in deionized solvent. However, in their criticism of the Langmuir model, Verwey and Overbeek[12] specifically stated that the counterions released by the colloidal particle do not contribute because the counterions reside in the vicinity of the macroion surface where the potential rapidly decays (p 40 of ref 12):

"Hence this part of the potential curve will have rather a small influence upon the form of the curve in the entire diffuse layer, as it comprises only a small part of the total space curve."

Thus, the counterions do not contribute to their own screening, and we have for the DLVO model the mathematical form that defines κ_{DLVO}

$$\kappa_{DLVO}^2 = 4\pi\lambda_B \sum_j Z_j^2 n_j = \kappa_{add}^2 \tag{6}$$

where n_j and Z_j are the average number density and the valency of the jth ionic species of the added salt, and the summation being over all the species. It is thus noted that in the Verwey-Overbeek assessment the counterions seem to have been lost since they are neither identified with the reduction in macroion charge as this would result in $Z_{eff} = 0$, nor do they contribute to κ as defined by eq 6.

However, if one were to insist that there is only one value of κ over the entire range of the separation distances, even to the region in which the van der Waals term becomes important, then one must include the counterions. The expression for the screening parameter currently employed by many does in fact include the released counterions but not the macroions, namely

$$\kappa^2 = \kappa_{add}^2 + \kappa_c^2 \tag{7}$$

where κ_c is defined by eq 5 and κ_{add} by eq 6. Thus, there is a coupling between κ and Z_p under low ionic strength conditions. One may also infer that a similar coupling also exists between the effective parameters κ_{eff} and Z_{eff}. Therefore, the parameters Z_{eff} and κ_{eff} are not independently adjustable parameters in the employment of the DLVO form of the pair potential between macroions.

3. Methods

3.1. MC Simulations and Characterization. The standard Wigner-Seitz spherical cell model is used in doing the canonical MC simulations. The macroion of radius a_p is fixed at the origin of the coordinate system. The cell radius a_{cell} is related to the macroion volume fraction ϕ_p by

$$a_{cell} = \left(\frac{1}{\phi_p}\right)^{1/3} a_p \tag{8}$$

For simplification the MC simulations are limited to "salt-free" conditions, which is taken to reflect the deionized solvent. The neutralizing counterions of common radius a_c are taken to be rigid ions moving in a dielectric continuum and occupying the macroion free volume

$$V_f = \frac{4\pi}{3}[a_{cell}^3 - (a_p + a_c)^3] \tag{9}$$

Thus the molar counterion concentration [c] (moles/liter) is given by

$$[c] = \frac{|Z_p/Z_c|}{\frac{4\pi}{3} a_{cell}^3 \left[1 - \phi_p\left(1 + \frac{a_c}{a_p}\right)^3\right] 1000 N_A} \tag{10}$$

where N_A is Avogadro's number and the distances are in meters.

Although the total number of configurations sampled in the simulations depended upon physical parameters such as the macroion charge and macroion volume fraction, about 10^6 to 10^7 configurations were used for equilibration of the system. The statistics of the system were then taken over the subsequent 10^8 to 10^9 configurations. An acceptance rate for the MC moves of approximately 50% was achieved by adjusting the displacement parameter for a move. The numerical procedure was tested by reproducing well-known spherical cell MC simulation results from the literature (see, for example, Wennerstörm et al. [15] and Bhuiyan et al.[16])

3.2. Analytical Expressions to Characterize the MC Results. The local number density of the counterions $n_c(r)$ obtained from the MC simulations is fitted to the analytical form,

$$n_c(r) = n_c g_c(r) = n_c(\infty) \exp(-\beta U_{pc}(r)) \tag{11}$$

The factor $n_c(\infty)$ in the analytical expression represents the number density in the limit $\beta U_{pc}(r) \rightarrow 0$ (i.e., the baseline value of $n_c(r)$). Thus, for consistency of the MC and analytical forms of analysis, we have

$$g_c(r) = \frac{n_c(\infty)}{n_c} \exp(-\beta U_{pc}(r)) = \exp(-A) \exp(-\beta U_{pc}(r)) \tag{12}$$

In the least-squares fitting of $g_c(r)$ obtained from the MC simulations the adjustable parameters for the analytical functional fit are A and those which define the screened Coulomb potential $\beta U_{pc}(r)$, which we next discuss.

The screened Coulomb pair potential in the single potential analysis is given by eq 3, where we write in terms of dimensionless parameters $x = r/a_p$ and $y_1 = \kappa_1 a_p$

$$\beta U_{pc}(r) = B_1 \frac{\exp(\kappa_1 a_p)}{1+\kappa_1 a_p} \frac{\exp(-\kappa_1 r)}{r} = B_1 \frac{\exp(y_1)}{1+y_1} \frac{\exp(-y_1 x)}{x} \tag{13}$$

where the subscripts indicate a single pair potential analysis. In some cases, however, a single pair potential was deemed to be inadequate. Under these circumstances, we take the logical step to write the pair distribution functions in terms of the sum of two screened Coulomb potentials

$$\beta U_{pc}(r) = B_f \frac{\exp(\kappa_f a_p)}{1+\kappa_f a_p} \frac{\exp(-\kappa_f r)}{(r/a_p)} + B_s \frac{\exp(\kappa_s a_p)}{1+\kappa_s a_p} \frac{\exp(-\kappa_s r)}{(r/a_p)}$$
$$= B_f \frac{\exp(y_f)}{1+y_f} \frac{\exp(-y_f x)}{x} + B_s \frac{\exp(y_s)}{1+y_s} \frac{\exp(-y_s x)}{x} \tag{14}$$

where f indicates the fast decay function and s the slow decay function. The adjustable parameters in the nonlinear least-squares fit are A_1, B_1, and y_1 for the single potential case; and A_2, B_f, y_f, B_s and y_s for the double exponential case, with the parameters A_1 and A_2 coming from the pre-factor of $\exp(-\beta U_{pc})$ (cf. eq 13) for the two cases, respectively. The set of dimensionless parameters B are identified with the effective charge(s) of the macroion, namely

$$B_1 = \frac{\lambda_B Z_1 Z_c}{a_p} \tag{15}$$

and

$$B_f + B_s = \frac{\lambda_B Z_f Z_c}{a_p} + \frac{\lambda_B Z_s Z_c}{a_p} \tag{16}$$

A measure of the validity of the screened Coulomb representation of the MC simulations with no added electrolyte is the degree to which the following expression is accurate

$$\kappa_j^2 = 4\pi\lambda_B Z_c^2 n_{c\kappa j} = 4\pi\lambda_B Z_c^2 |Z_{\kappa j}| \left(\frac{\phi_p}{V_p}\right) \tag{17}$$

where $V_p = (4\pi/3)a_p^3$ is the volume of the macroion. In the case of the single pair potential $\kappa_j = \kappa_1$ and for the two pair potential κ_j is either κ_f or κ_s. There is no constraint to force Z_{κ_1} to be equal to Z_1, or to force Z_{κ_j} to be equal to the corresponding effective charges calculated from either B_f or B_s.

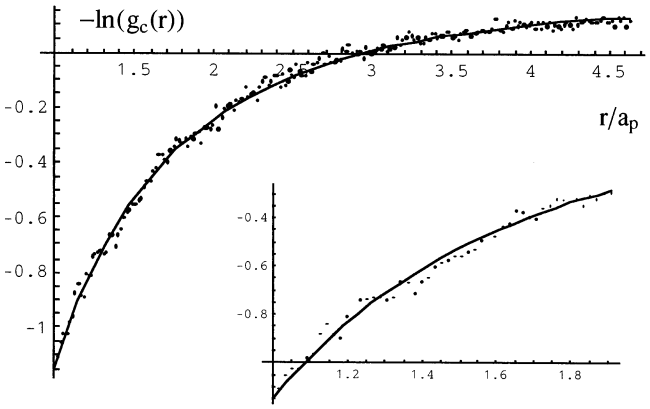

Figure 1. Single pair potential analysis of $-\ln(g_c(r))$ Versus r/a_p for Monovalent Counterions. The parameters in the MC simulations were $a_p = 113 \times 10^{-10}$ m, $a_c = 1 \times 10^{-10}$m, $Z_p = 30$, $Z_c = -1$, and $\phi_p = 0.03$. The least squares parameters for the single pair potential analysis shown by the solid line are $A_1 = 0.191$, $B_1 = -1.938$, and $y_1 = 0.788$. The insert is the first 50 points.

3.3. Least Squares Analysis. The nonlinear least-squares analysis method used in this study for both the single and double screened Coulomb potential forms is summarized in the Appendix. In all cases, the initial guess parameters were internally estimated by the program. Iterations were continued until all of the adjustable parameters were changed by less than 0.1% of its previous value.

4. Results and Discussion

In all of the reported calculations we have used the parameters $a_p = 113 \times 10^{-10}$ m, $a_c = 10^{-10}$ m, $T = 298$ K, and $\epsilon_r = 78.5$. These parameters or very similar ones have been used earlier in the literature[8,10] for such systems. We begin this discussion by analyzing the qualitative and quantitative features of the least-squares fit to the MC simulations. Later, we will discuss some recent relevant experimental work in the light of the present work.

4.1. Quality of the MC Simulations and Least Squares Fit. The quality of the MC simulations and the nonlinear least squares curve fitting are assessed in the curves $-\ln(g_c(r))$ versus $x = r/a_p$. Shown in Figure 1 are the results for $Z_p = 30$, $Z_c = -1$, and $\phi_p = 0.03$, where in the least-squares analysis, a single exponential has been used in the pair potential. The top curve is for the full data set and the lower curve is the first fifty data points in expanded form to emphasize the early decay range. The statistics in the MC simulations are reflected in the scatter in the points in the $-\ln(g_c(r))$ function. The parameters in the least squares curve (solid lines) are $A_1 = 0.191$, $B_1 = -1.938$, and $y_1 = 0.788$. Attempts to fit these data with a two-exponential pair potential function failed. Thus, for low charge the single-exponential pair potential appears to be sufficient in the characterization of the entire data set.

We show in Figure 2 the curves for $Z_p = 400$, $Z_c = -1$, and $\phi_p = 0.01$ for the single exponential pair potential model. The MC statistics are much improved over that in Figure 1 as indicated by the reduced scatter in the simulated points. It is quite clear that a single pair screened interaction does not adequately fit the entire range of data points. The parameters in the least squares function are $A_1 = 1.500$, $B_1 = -12.83$, and $y_1 = 0.931$. The results for the double exponential pair interaction model on this MC function are shown in Figure 3. The parameters that generated the solid line are $A_2 = 1.600$, $B_f = -13.679$, $B_s = -10.324$, $y_f = 8.444$, and $y_s = 0.721$. The fit

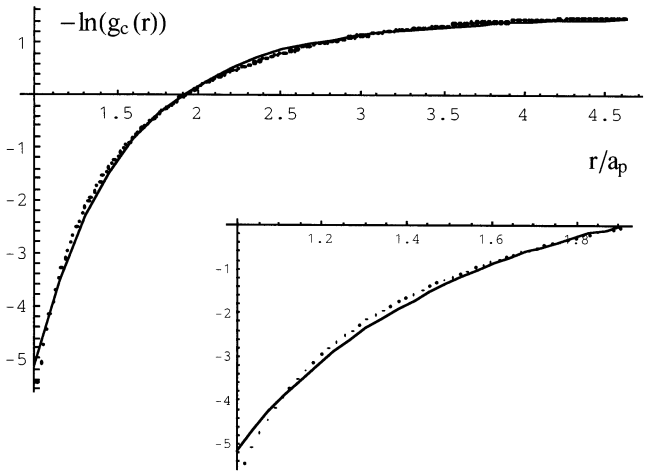

Figure 2. Single pair potential analysis of $-\ln(g_c(r))$ Versus r/a_p for Monovalent Counterions. The parameters in the MC simulations were $a_p = 113 \times 10^{-10}$ m, $a_c = 1 \times 10^{-10}$m, $Z_p = 400$, $Z_c = -1$, and $\phi_p = 0.01$. The least squares parameters for the single pair potential analysis shown by the solid line are $A_1 = 1.500$, $B_1 = -12.83$, and $y_1 = 0.931$. The insert is the first 50 points.

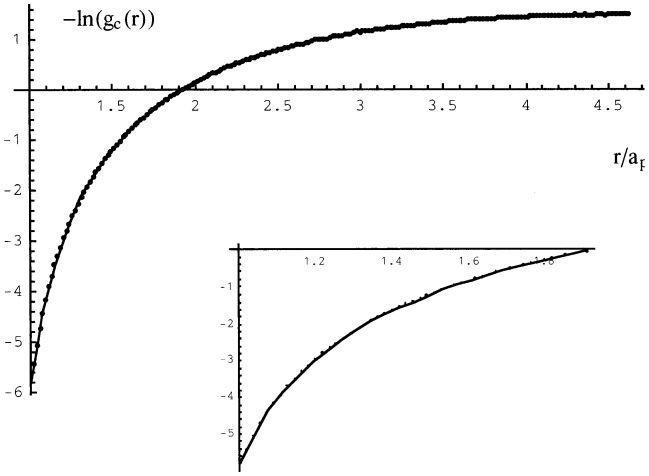

Figure 3. Double pair potential analysis of $-\ln(g_c(r))$ Versus r/a_p for monovalent counterions. The parameters in the MC simulations were $a_p = 113 \times 10^{-10}$ m, $a_c = 1 \times 10^{-10}$m, $Z_p = 400$, $Z_c = -1$, and $\phi_p = 0.01$. The least squares parameters for the single pair potential analysis shown by the solid line are $A_2 = 1.600$, $B_f = -13.679$, $B_s = -10.324$, $y_f = 8.444$, and $y_s = 0.721$. The insert is the first 50 points.

of the data with this double exponential potential model is visually very good.

Attention is now directed to divalent counterions simulations. Shown in Figure 4 are the results for $Z_p = 50$, $Z_c = -2$, and $\phi_p = 0.04$. The solid line was generated with the single-exponential pair interaction using the parameters $A_1 = 0.6494$, $B_1 = -6.219$, and $y_1 = 1.129$. As in the low charge case with monovalent counterions, attempts to fit the MC curves of low macroion charge to the double exponential functionagain failed.

We next display the results for an increase in charge of the macroion. Shown in Figure 5 are the results for $Z_p = 250$, $Z_c = -2$, and $\phi_p = 0.04$. The statistics of the MC simulations are greatly improved due to the larger number of counterions. The parameters for the single-exponential screened Coulomb potential model are $A_1 = 1.742$, $B_1 = -18.090$, and $y_1 = 1.981$. The solid curve does not represent a good fit of the simulated distribution function obtained by MC methods.

The double exponential screened Coulomb model was fit to the MC distribution function for $Z_p = 250$, $Z_c = -2$, and $\phi_p = 0.04$ and shown in Figure 6. The parameters for the double

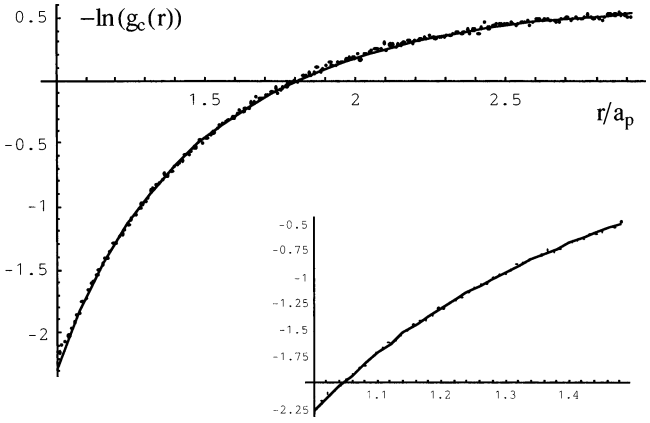

Figure 4. Single pair potential analysis of $-\ln(g_c(r))$ versus r/a_p for divalent counterions. The parameters in the MC simulations were $a_p = 113 \times 10^{-10}$ m, $a_c = 1 \times 10^{-10}$m, $Z_p = 50$, $Z_c = -2$, and $\phi_p = 0.04$. The least squares parameters for the single pair potential analysis shown by the solid line are $A_1 = 0.6494$, $B_1 = -6.219$, and $y_1 = 1.129$. The insert is the first 50 points.

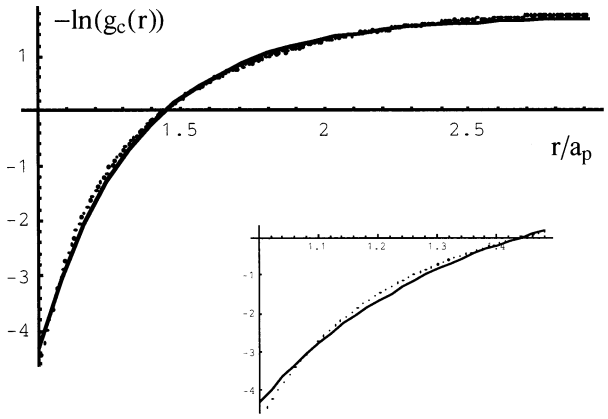

Figure 5. Single pair potential analysis of $-\ln(g_c(r))$ versus r/a_p for divalent counterions. The parameters in the MC simulations were $a_p = 113 \times 10^{-10}$ m, $a_c = 1 \times 10^{-10}$m, $Z_p = 250$, $Z_c = -2$, and $\phi_p = 0.04$. The least squares parameters for the single pair potential analysis shown by the solid line are $A_1 = 1.742$, $B_1 = -18.090$, and $y_1 = 1.981$. The insert is the first 50 points.

exponential potential function least-squares fit are $A_2 = 1.887$, $B_f = -17.419$, $B_s = -12.093$, $y_f = 9.062$, and $y_s = 1.403$. The fit of the MC function with this double potential model is visually very good over the entire range of points.

The philosophy behind the above analysis is that if the screened Coulomb form of the pair potential, whether the single or double form, is correct then the two charges Z_j and Z_{κ_j} would be equivalent. For completeness we compare the results in which both charges are allowed to float to the case when Z_j is forced to be equivalent to Z_{κ_j}. That is, the only adjustable parameters are A_j and Z_j. This comparison was carried out for the low charge case of $Z_p = 50$ and $\phi_p = 0.04$ to ensure only one exponential decay and adequate statistics in the MC simulations. In the case when both charges are allowed to float the characteristic parameters were found to be $A_1 = 0.3394$ with $\exp(-A_1) = 0.712$; $Z_1 = 52.808$; and $Z_{\kappa_1} = 137$. In the case when the two charges were "forced" to be equivalent we obtained "slightly" imaginary numbers $Z_1 = Z_{\kappa_1} = 42.9159 + 1.821 \times 10^{-5}\, i$ and $A_1 = 0.509372 + 1.7124 \times 10^{-7}\, i$. Taking only the real part of the "forced" fit analysis the two methods of fit are compared in Figure 7. It is quite evident that the "floating" method provides the better fit.

We can generalize the least-squares fit to screened Coulomb pair interactions to our MC simulations of $g_c(r)$, using a visual

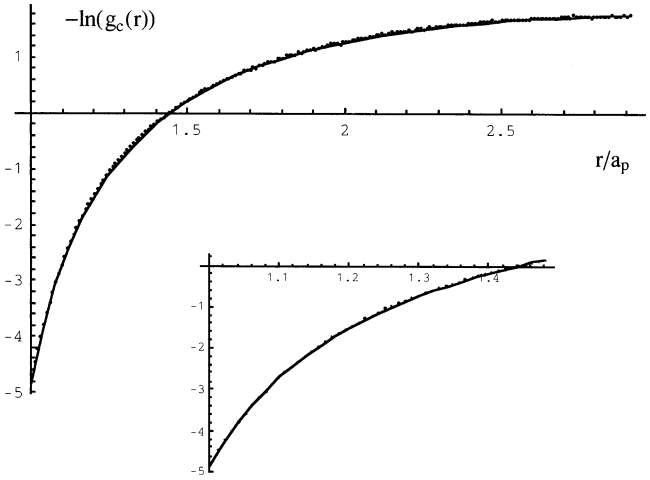

Figure 6. Double pair potential analysis of $-\ln(g_c(r))$ versus r/a_p for monovalent counterions. The parameters in the MC simulations were: $a_p = 113 \times 10^{-10}$ m, $a_c = 1 \times 10^{-10}$m, $Z_p = 250$, $Z_c = -2$, and $\phi_p = 0.04$. The least squares parameters for the single pair potential analysis shown by the solid line are $A_2 = 1.887$, $B_f = -17.419$, $B_s = -12.093$, $y_f = 9.062$, and $y_s = 1.403$. The insert is the first 50 points.

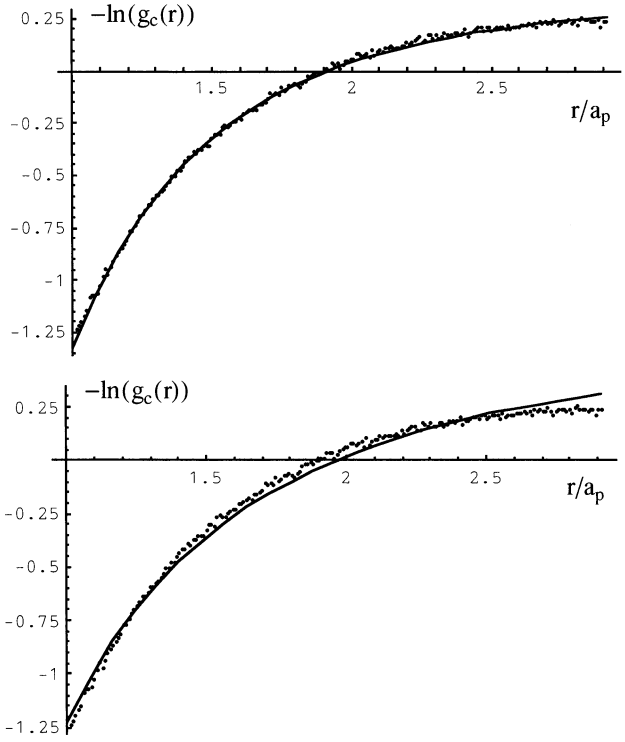

Figure 7. Comparison of "Floating" and "Forced" Fit Analysis of $-\ln(g_c(r))$. MC simulations were performed with $Z_c = -1$, $Z_p = 50$, and $\phi_p = 0.04$. The top figure is the data and the least-squares fit using the "floating" parameter method. The solid line is the single screened pair potential using the parameters $A = 0.3394$ with $\exp(-A) = 0.712$, $Z_1 = 52.808$, and $Z_{\kappa_1} = 137$. The "forced" fit analysis of the same MC data yielded "slightly" imaginary numbers $Z1 = Z_{\kappa_1} = 42.9159 + 1.821 \times 10{-}5i$ and $A1 = 0.509372 + 1.7124 \times 10{-}7i$. The bottom figure is the MC data and the least squares curve using only the real part of $Z1$ and A, for which $\mathrm{Re}[Z1] = 42.92$, $\mathrm{Re}[\kappa_1] = 5062\ \mathrm{m}^{-1}$, $\mathrm{Re}[A] = 0.509372$ and $\exp(-\mathrm{Re}[A]) = 0.6009$.

inspection as a means of determination of the "quality of fit". In the case of low macroion charge a single exponential pair interaction is quite adequate. Attempts to use the double exponential model did not converge as the inversion of the matrix G in eq (A6) (cf., Appendix) led to ill-behaved conditions. We do not believe that the inability to fit the MC simulations with the double potential model is due to the relatively poor statistics in the MC simulations. Rather, the inability to fit these low charge distribution functions with the double pair interaction model is due either to the fact that only one exponential is present or that there is no discernible difference between multiple pair potentials if they do in fact exist. In other words, there is only one population of counterions for low charge macroion systems whereas at least two classes exist for the higher charged macromolecular species.

TABLE 1: Charge Characterization of MC Simulations for Monovalent Counterion

ϕ_p	Z_p	Z_1	Z_f	Z_s	$\exp(-A_1)$	$\exp(-A_2)$	$g_c(a_{cell})$[a]
0.01	30	30.5			0.826		0.8909
0.03	30	31.4			0.806		0.8658
0.05	30	32			0.806		0.8617
0.001	50	50.4			0.834		0.8844
0.01	50	51.4			0.745		0.8209
0.04	50	52.8			0.712		0.7921
0.001	150	124.8			0.558		0.4935[b]
0.01	150	126.6			0.460		0.5077
0.04	150	134.8			0.439		0.4930
0.03	150	133.1			0.440		0.4955
0.001	250	156.2			0.391		0.4140
0.04	250	189.2			0.316		0.3499
0.01	400	201.9	215.3	162.5	0.223	0.202	0.2274
0.03	1000	317.8	663.4	211.7	0.102	0.086	0.0969
0.05	1000	363.4	698.8	237.3	0.106	0.089	0.102

[a] The functions $\exp(-A1)$ and $\exp(-A2)$ represent the hypothetical value $g_c(r \rightarrow \infty)$, whereas this is last point in the MC determined distribution function at $r = a_{cell}$. [b] Low value is attributed to statistical error in simulation (see text).

TABLE 2: Kappa Characterization of MC Simulations for Monovalent Counterions

ϕp	Zp	$Z_{\kappa 1}$	$Z_{\kappa f}$	$Z_{\kappa s}$	$[c_{\kappa_1}]/10^{-3}$	$[c_{\kappa_f}]/10^{-3}$	$[c_{\kappa_s}]/10^{-3}$
0.01	30	103.3			0.284		
0.03	30	108.7			0.896		
0.05	30	120.0			1.65		
0.001	50	137.2			1.51		
0.01	50	140.8			0.387		
0.04	50	137.2			1.508		
0.001	150	323.7			0.089		
0.01	150	256.0			0.704		
0.04	150	231.0			2.540		
0.03	150	235.4			1.94		
0.001	250	473.9			0.130		
0.04	250	316.1			3.475		
0.01	400	454.9	37407	272.4	1.25	103	0.748
0.03	1000	625.3	36391	297.2	5.16	300	2.45
0.05	1000	642.5	28194	314.3	8.83	387	4.32

4.2. Quantitative Characterization of the Least Squares Fit Parameters. MC simulations provide a standard by which to test the analytical theories in regard to the validity and interpretation of the "adjustable" fit parameters. We will now attempt to place physical interpretations on the numerical values of the "best fit" parameters for both the single and double exponential screened Coulomb pair interaction potential models. We will separate our analysis into two parts. The first part focuses on the "extremes" of the $g_c(r)$ function, namely, B_1, B_f, and B_s and also $\exp(-A_1)$ and $\exp(-A_2)$. The second part addresses the "rate of decay" of the distribution function as manifested in the parameters y_1, y_f, and y_s.

The numerical values of the "best fit" parameters for monovalent counterions are given in Tables 1 and 2. The dashed lines indicate that two decay functions could not be discerned in the double screened Coulomb case. It is observed that for these low charge colloidal particles the value of Z_1 is very close to the value of Z_p employed in the MC simulations. Deviations

from this apparent equality of parameters begin around $Z_p = 150$. Within the context of the current trend the values of $Z_1 < Z_p$ would be considered as "effective charges". Because there is no added electrolyte Z_{κ_1} may be calculated from eq 16 and directly compared with the "effective charge" Z_1. In all cases given in Tables 1 and 2 we have $Z_1 < Z_{\kappa_1}$. What this means is that the values of the screening parameters, hence, the "effective" free ion concentrations, in these simulations are larger than expected on the basis of Z_1 alone. Let us now compare these inequalities with the "bare" charge in the simulations. The trend in the data in Table 2 is $Z_{\kappa_1} > Z_p$ for the "weaker" macroion charges. Thus the "apparent ionic strength" is above the upper bound based on the number of counterions in the system. From the experimental point of view such an inequality would be interpreted as an "impurity" that might arise from dissolved gases, for example. The inequality is reversed when $Z_p = 1000$. Such behavior obtains if there is an underlying "rapid" decay rate that is present in the decay of the counterion cloud. That is, the single set of fitting parameters attempts to represent both decay curves. When $Z_p = 1000$ the region of the counterion cloud that has the fast decay rate has sufficiently collapsed to the vicinity of the macroion surface that the slower decay rate dominates the analysis. This is similar to the view of Verwey and Overbeek[12] in the above quote. Still, however, the inequalities $Z_{\kappa f}$ and $Z_{\kappa s}$ persist in the two-decay analysis.

Because the least-squares fit is over the entire range of MC data, one has by definition the approximate relationship $g_c(a_{cell}) = \exp(-A)\exp(-\beta U_{pc}(a_{cell}))$ for either the single or double exponential pair potential form. In theory, the inequality $\exp(-A) < g_c(a_{cell})$ is obtained if the range of influence of the macroion extends beyond the distance a_{cell}. It is noted, however, that in practice some limited cases result in values of $\exp(-A_1)$ and $\exp(-A_2)$ that lie below the values of $g_c(a_{cell})$. This apparent discrepancy is easily explained in terms of the larger statistical error for the very dilute systems. For example, in the particular case for $\phi_p = 0.001$ and $Z_p = 150$ the last five values of $g_c(r)$ are 0.6077, 0.6051, 0.6158, 0.6201, and 0.4935. It may be concluded that the "true" value of $g_c(a_{cell})$ is in the vicinity 0.60 rather than the obtained value of 0.4935. Another characteristic of the values of $\exp(-A_j)$ is that it is more closely equated with $g_c(a_{cell})$ as the charge of the macroion increases. This is consistent with the notion that the higher charged macroion draws the counterion closer to its surface, which increases the effect of screening and thus reduces the range of the macroion influence. This also means that the finer details of the counterion distribution about a macroion are lost at sufficient distances from the macroion.

Although the general characteristics of the divalent data summarized in Tables 3 and 4 follow the trends for the monovalent counterions, there are some very significant differences. Two important similarities are that $g_c(r)$ for the lowest charge macroion can only be fit by the single screened Coulomb model, and that the values of $\exp(-A)$ are virtually identical for a given charge Z_p and for either the single or double exponential pair potential model. It is observed, however, that the values of $\exp(-A)$ become significantly smaller when the divalent counterion is substituted for the monovalent counterion. The physical interpretation is that the divalent counterions are more strongly drawn to the macroion than are the monovalent counterions. Consistent with this interpretation is the observation that the double exponential screened Coulomb interaction model can be applied to the $Z_p = 150$ data whereas this model resulted in ill conditioned matrixes for the monovalent case in the matrix inversion procedure.

TABLE 3: Charge Characterization of MC Simulations for Divalent Counterions

ϕp	Zp	Z_1	Z_f	Z_s	$\exp(-A_1)$	$\exp(-A_2)$	$g_c(a_{cell})^a$
0.001	50	47			0.682		0.7509
0.040	50	49			0.522		0.6010
0.001	150	84	66	72	0.336	0.309	0.3372
0.010	150	94	67	75	0.276	0.247	0.2801
0.040	150	109	54	90	0.261	0.243	0.2769
0.050	150	89	70	72	0.287	0.260	0.2924
0.001	250	94	139	77	0.214	0.192	0.2108
0.040	250	142	137	95	0.175	0.151	0.1735
0.050	500	122	331	82	0.099	0.084	0.09215
0.010	900	149	614	83	0.055	0.043	0.0471
0.050	900	130	592	80	0.057	0.046	0.0490

[a] The functions $\exp(-A1)$ and $\exp(-A_2)$ represent the hypothetical value $g_c(\infty)$ whereas this is the last point in the MC-determined distribution function at $r = a_{cell}$.

TABLE 4: Kappa Characterization of MC Simulations for Divalent Counterions

ϕp	Zp	$Z_{\kappa 1}$	$Z_{\kappa f}$	$Z_{\kappa s}$	$[c_{\kappa_1}]/10^{-3}$	$[c_{\kappa_f}]/10^{-3}$	$[c_{\kappa_s}]/10^{-3}$
0.001	50	59			0.016		
0.040	50	49			0.459		
0.001	150	149	28864	84	0.041	7.9	0.023
0.010	150	105	4802	62	0.289	13.2	0.170
0.040	150	90	2317	64	0.995	25.5	0.705
0.050	150	12	836	7	0.160	11.5	0.092
0.001	250	194	4937	91	0.053	13.6	0.025
0.040	250	129	2693	65	1.41	29.6	0.710
0.050	500	22	2639	8	0.295	36.0	0.112
0.010	900	250	24922	71	0.686	68.5	0.196
0.050	900	26	4365	8	0.35	60.0	0.107

4.3. Analysis of Experimental Data on Macroion Pair Potential. There is a current trend to fit experimental data to the form of a screened Coulomb pairwise interaction. In this form of the pair potential there are three characteristic parameters: the macroion charge Z_p, the macroion radius a_p, and the screening parameter κ. If the set of characteristic parameters have values identical to, or nearly identical to, the anticipated values obtained from other measurements, then one is believed justified in the conclusion that the pair potential accurately depicts the pairwise interaction. However, if the set of characteristic parameters differ greatly from those of anticipation, then one is faced with two possible interpretations. First, the screened Coulomb form is not a very good representation of the interactions that take place in the system. One must then conclude that there is no physical content in the numerical values of Z_p, a_p, and κ, and therefore it would be meaningless to compare results on different systems. The second choice is that there is physical content of the characteristic parameters and their values are to be taken as "effective" parameters. It is not clear, however, if one set of effective parameters under one set of conditions can be compared with another set of effective parameters obtained under a different set of circumstances. It is thus left to theorists to find some "bridge" between the two (or more) sets of characteristic parameters. This is apparently the position of Ulander, Greberg, and Kjellander[11] in the above quotation, with the goal to further the use of the simple form of a screened Coulomb potential between charges species.

However complex the method of analysis to provide justification of endorsement of the "effective" characteristic parameters, the situation only worsens if there is no relationship between these parameters.

Nevertheless, experimentally determined values of κ_{eff} have been used to interpret data. As an example, we turn to Tata-Ise[17,18] /Grier-Crocker[19] "controversy" regarding the determination of the pair distribution function using optical tweezer

methods.[20,21] The controversy centers on whether the Sogami-Ise (SI) pair potential[22] or the DLVO potential describes the interaction between particle pairs. The controversy itself is of no relevance to the present study, so it is sufficient to state that the SI potential has a long-range attractive tail that is not present in the DLVO theory. What is relevant is the experimental system and the subsequent analysis of both the SI and DLVO pair potentials in terms of "free floating " parameters Z_{eff} and κ_{eff} in our notation. The experimental system was composed of a mixture of colloidal spheres of radii $a_{\text{p}} = 0.325$, 0.485, and 0.765-μm in distilled water. The six combinations of pairs were isolated by optical tweezer methods and their relative positions were monitored, from which a pair distribution function was constructed. For the SI potential, they reported that $1/\kappa_{\text{eff}} = 957$ nm for $a_{\text{p}} = 0.765$ μm and noted that this value was "within experimental error of the theoretical upper limit set by the dissociation of water itself" and is therefore "experimentally difficult" to obtain. By making this comparison with pure water, they acknowledge that κ_{eff} is *intended to have direct physical significance*. This being the case, we can freely associate their values of κ_{eff} reported for the DLVO fit as *likewise having direct physical significance* in an attempt to deduce further properties about their experimental conditions. We may therefore write for the screening parameter for their system a the multi-macroion extension of eq 5

$$\kappa^2 = 4\pi\lambda_B(n_1 + n_2 + n_3 + n_i) \tag{18}$$

where $n_1 = |Z_1|n_{\text{p1}}$, $n_2 = |Z_2|n_{\text{p2}}$, and $n_3 = |Z_3|n_{\text{p3}}$ are the number densities of the released univalent counterions for the colloidal particles of number densities n_{p1}, n_{p2}, and n_{p3}. The number density n_i accounts for the contribution of all other ions, including those that arise from the dissociation of the solvent. The values of $1/\kappa_{\text{eff}}$ were reported to be 272:268:289 nm for the effective charge values $Z_{\text{eff}} = Z_1/Z_2/Z_3$ of 6000:13 800:22 800. To check whether Z_{eff} and κ_{eff} can be varied independently would require independent knowledge of the densities n_{p1}, n_{p2}, n_{p3}, and n_i. Unfortunately, this information is not available. However, information is given in Grier and Crocker[19] that might allow one to estimate the validity of eq 1. According to them, the value of κ_{eff} obtained from their DLVO fits corresponds to an ionic strength of 1.2 μM and pure water has an ionic strength of 0.97 μM. Therefore, if the solvent contains no other ions, the ionic strength attributed to the counterions is 0.23 μM, or a concentration of univalent counterions of $C_s = 2I_s = 0.46$ μM, or $n_{\text{c}} \cong 2.8 \times 10^{20}$ counterions/m^3. Because neither the absolute nor the relative concentrations of the three latex preparations is known, we can use the value of n_{c} for colloidal particles having the largest charge to estimate the maximum value of the average separation distance between these particles, d_{max}. The maximum value is $(Z/n_{\text{c}})^{1/3} = (22\,800/(2.8 \times 10^{20}))^{1/3} = 4.35 \times 10^{-6}$m, or 4.35 μm $= d_{\text{max}}$. However, the range of distances given in Figure 1 of Grier and Crocker[19] indicates there *is no spatial correlation between two spheres up to a distance of 7 μm.* If one insists on placing *reliable physical significance in their numerical value of* κ_{eff}, then either a "dense" phase outside the range of their observation exists to allow unimpeded distances up to 7 μm $> d_{\text{max}}$ (two-state structure), or one could speculate that their "deionized" water is contaminated. The alternative interpretation is that κ_{eff} no more reflects the "true" screening parameter than Z_{eff} gives an accurate value for the "bare charge" Z_{p}. In this regard, it is difficult to employ real experimental data because there are too many unknowns about the composition of the medium. For example, dissolved carbon dioxide represents an unknown in regard to the ionic composition of the solution.

5. Concluding Remarks

The main achievement of this paper has been an examination of the nature of the ion-cloud around a macroion in a charge stabilized suspension in the light of the screened-coulomb potential approach. The macroion−microion radial distribution function $g_{\text{c}}(r)$ has been fitted to its MC-simulated counterpart, with the screened-coulomb potential being approximated by a single or two exponential screened Coulomb form of the pair interaction potential. It is a generally accepted premise that computer simulations often provide a more reliable assessment of the application of analytical expressions such as screened Coulomb interactions than real experimental data. The reasons are implicit in the discussion in the previous section. We should emphasize, however, that the goal of the present exercise has been to gather insight into the character of this counterion cloud rather than merely the fitted parameters.

The MC simulations in the present study, when characterized by one or two screened Coulomb pairwise interactions, clearly indicate two "populations" of counterions for macroions of sufficiently high charge. These populations are distinguished solely on the basis of different "rates" of decay of their distributions when one moves away from the macroion. These rates are represented by two different values of κ in the description of the "shape" of the pair distribution function $g_{\text{c}}(r)$. This "bimodal" distribution is consistent with the Brownian dynamics (BD) simulations of Sanghiran and Schmitz[8], in which the time course of the individual counterions are tracked. In the BD simulations, the counterions were found to freely roam the entire volume of the simulation cell for low charge density macroions. However, as the macroion charge was increased, the counterions were found to remain in the vicinity of the macroion after having achieved the "equilibrium" configuration. In the present MC simulations also, at high Z_{p}, the inner counterions are found to be highly collapsed nearer to the macroion surface and are responsible for most of the screening of the macroion charge, while the outer counterions that are more removed from the macroion surface, are more diffused. Such bimodal distributions of counterions is reminiscent of "condensation" models of rodlike polyions such as in the Manning theory. However, we must reiterate that the counterions in our simulations are not actually partitioned into two such distinguishable populations. Rather, we interpret the necessity of two different κ values as an indication that the shape of the pair distribution function is not a single, smoothly varying function with distance. In this regard, one might not expect the values of κ_f and κ_s to be independent of either the macroion charge or the valency of the counterion.

As indicated in the Introduction, the screened-Coulomb notion pioneered by the DLVO theory is intuitively simple and coupled with its ease of use has made it a popular technique for quick and routine analysis of many experimental data. Our study suggests that the use of more than one exponential in the screened − Coulomb potential would probably be more useful at high macroion charges, especially in the presence of multivalent counterions.

Appendix: Least Square Method

The numerical analysis of data is a common task in science. Under normal circumstances, the least-squares analysis technique is not generally presented in detail, as these programs may be found as software packages. What is at issue in this

study is the least-squares analysis of the pair distribution function and subsequent assessment of the physical content of the fitting parameters. Hence, the least squares procedure should be made bare to the reader.

The principle behind a least-squares analysis is to minimize the difference between the real experimental data and a particular mathematical form. We define the quantity S as

$$S = \sum_{i=1}^{N} (D_i - F_i)^2 \tag{A1}$$

where D_i is the actual i-th data point and F_i is the value of the mathematical function for the i-th point. Let us write $F = F[\{\alpha\},r]$, where $\{\alpha\}$ is the set of parameters $\{A_1, B_1, y_1\}$ for the one-potential or $\{A_2, B_f, y_f, B_s, y_s\}$ for the two-potential fit of the function $g_c(r)$ in eq 16. To minimize S, one takes the derivative with respect to all of the adjustable parameters

$$\frac{\partial S}{\partial \alpha} = \sum_{i=1}^{N} (D_i - F_i)\left(\frac{\partial F_i}{\partial \alpha}\right) = 0 \tag{A2}$$

For the nonlinear expression, the function F itself is expressed as a Taylor series expansion to improve upon a previously employed set of parameters. That is, the values of the parameters for the $k+1$ cycle are based on their values on the k-th cycle

$$F^{k+1} = F^k + \sum_{\gamma} \left(\frac{\partial F}{\partial \gamma}\right)_{\gamma=\gamma^k} \Delta\gamma \tag{A3}$$

where $\Delta\gamma = \gamma^{k+1} - \gamma^k$ is the residual of the γ variable. Hence, the minimization expression is now written as

$$\sum_{\alpha} \frac{\partial S}{\partial \alpha} = \sum_{\alpha} \sum_{i=1}^{N} \left(D_i - \left(F_i^k + \sum_{\gamma} \left(\frac{\partial F_i}{\partial \gamma}\right)_{\gamma=\gamma^k} \Delta\gamma\right)\right)\left(\frac{\partial F_i}{\partial \alpha}\right)_{\alpha=\alpha^k} = 0 \tag{A4}$$

We now reorganize the order of summation and express the result in terms of matrix multiplication notation

$$\sum_{\alpha} \left[\sum_{i=1}^{N} (D_i - F_i^k)\left(\frac{\partial F_i}{\partial \alpha}\right)_{\alpha=\alpha^k}\right] - \sum_{\alpha} \sum_{\gamma} \left[\sum_{i=1}^{N} \left(\frac{\partial F_i}{\partial \alpha}\right)_{\alpha=\alpha^k}\left(\frac{\partial F_i}{\partial \gamma}\right)_{\gamma=\gamma^k}\right]\Delta\gamma = T - \boldsymbol{G}\cdot\boldsymbol{R} = 0 \tag{A5}$$

The elements of the matrix $\boldsymbol{G}$ are defined as

$$(\boldsymbol{G})_{\alpha\gamma} = \sum_{i=1}^{N} \left(\frac{\partial F_i}{\partial \alpha}\right)_{\alpha=\alpha^k}\left(\frac{\partial F_i}{\partial \gamma}\right)_{\gamma=\gamma^k} \tag{A6}$$

The elements of the vector $\boldsymbol{T}$ are given as

$$(\boldsymbol{T})_{\gamma} = \sum_{i=1}^{N} (D_i - F_i^k)\left(\frac{\partial F_i}{\partial \gamma}\right)_{\gamma=\gamma^k} \tag{A7}$$

and the elements of the vector of residuals $\boldsymbol{R}$ are identified as

$$(\boldsymbol{R})_{\gamma} = \Delta\gamma = \gamma^{k+1} - \gamma^k \tag{A8}$$

Hence, the "new guess" for the parameter β involves a matrix inverse

$$\gamma^{k+1} = \gamma^k + (\boldsymbol{G}^{-1}\cdot\mathbf{T})_{\beta} \tag{A9}$$

where the Gauss-Jordan method was used to find the inverse matrix. This is repeated until a value of $|\Delta\gamma/\gamma| < 0.001$ is obtained for each γ.

Acknowledgment. Partial support of an NSF Grant 0137273 is acknowledged. L.B.B. also acknowledges an institutional grant through FIPI, University of Puerto Rico.

References and Notes

(1) Roberts, J. M.; O'Dea, J. J.; Osteryoung, J. G. *Anal. Chem.* **1998**, *70*, 3667−3673.
(2) Alexander, S.; Chaikin, P. M.; Grant, P.; Morales, G. J.; Pincus, P.; Hone, D. *J. Chem. Phys.* **1984**, *80*, 5776.
(3) Stevens, M. J.; Falk, M. L.; Robbins, M. O. *J. Chem. Phys.* **1996**, *104*, 5209, 5219.
(4) Gisler, T.; Schulz, S. F.; Borkovec, M.; Sticher, H.; Schurtenberger, P.; D'Aguanno, B.; Klein, R. *J. Chem. Phys.* **1994**, *101*, 9924.
(5) Belloni, L. *Colloids Surf.* **1998**, *140*, 227.
(6) Linse, P. *J. Chem. Phys.* **2000**, *113*, 4359.
(7) Shklovskii, B. I. *Phys. Rev. E* **1999**, *60*, 5802.
(8) Sanghiran, V.; Schmitz, K. S. *Langmuir* **2000**, *20*, 7566, 7574.
(9) Schmitz, K. S. *Langmuir* **2000**, *16*, 2115, 2123.
(10) Mukherjee, A. K.; Schmitz, K. S.; Bhuiyan, L. B. *Langmuir* **2002**, *18*, 4210, 4219.
(11) Ulander, J.; Greberg, H.; Kjellander, R. *J. Chem. Phys.* **2001**, *115*, 7144−7160.
(12) Verwey, E. J.; Overbeek, J. T. G. *Theory of the Stability of Lyophobic Colloids*; Elsevier Publishing Co., Inc.: New York, 1948.
(13) Langmuir, I. *J. Chem. Phys.* **1938**, *6*, 873, 896.
(14) Chan, D. Y. C.; Linse, P.; Petris, S. N. *Langmuir* **2001**, *17*, 4202, 4210.
(15) Wennerstörm, H.; Jönsson, B.; Linse, P. *J. Chem. Phys.* **1982**, *76*, 4665.
(16) Bhuiyan, L. B.; Outhwaite, C. W.; Bratko, D. *Chem. Phys. Lett.* **1992**, *193*, 203.
(17) Tata, B. V. R.; Ise, N. *Phys. Rev. E* **1998**, *58*, 2237.
(18) Tata, B. V. R.; Ise, N. *Phys. Rev. E* **2000**, *61*, 983−985.
(19) Grier, D. G.; Crocker, J. C. *Phys. Rev. E* **2000**, *61*, 980−982.
(20) Crocker, J. C.; Grier, D. G. *Phys. Rev. Lett.* **1994**, *73*, 352.
(21) Crocker, J. C.; Grier, D. G. *Phys. Rev. Lett.* **1996**, *77*, 1897−1900.
(22) Sogami, I.; Ise, N. *J. Chem. Phys.* **1984**, *81*, 6320−6330.